OUTER AND INNER SURFACE FLAWS IN THICK-WALLED PRESSURE VESSELS

S. N. ATLURI, K. KATHIRESAN

School of Engineering Science and Mechanics,
Geogia Institute of Technology,
225 North Avenue, N.W., Atlanta, Georgia 30332, U.S.A.

SUMMARY

The objective of this paper is to present the results for stress-intensity factors (SIF), directly computed through a three-dimensional, embedded singularity, hybrid-displacement finite element procedure, for semi-elliptical cracks, of various geometries, located at the outer or inner surfaces of pressurized or thermally shocked thick walled cylinders.

The only available estimates for SIF in the present class of problems are due to Kobayashi *et al.* (paper G 4/3, 3rd SMiRT) based on the conjecture that the SIF for surface flaws in cylinders can be estimated from SIF's for surface flaws of similar geometry in flat plates and the "curvature-correction factors" obtained from simple two-dimensional analogs. This estimation procedure has been argued, in subsequent literature, to be questionable for deep surface flaws in thick-walled pressure vessels. This motivated the present computations, which involve no restrictive assumptions.

In the present paper, an embedded singularity, fully three-dimensional hybrid-displacement finite element model, as applied to linear fracture analysis, the theoretical development of which is given in Atluri *et al.* (paper L 7/3, 3rd SMiRT), is employed to directly compute SIF's in the above class of problems. The developed hybrid-displacement model is based on a modified variational principle of total potential energy with three independently assumed field variables, which are: (a) an arbitrary displacement field u in the interior of each element in which, in the case of elements near the crack front, the asymptotically correct $\sqrt{r}$ type analytical solution is embedded; (b) an inherently compatible interelement-boundary displacement field; v; and (c) a boundary traction field (Lagrange Multiplier) which is used to enforce the boundary displacement compatibility condition, $u=v$ at the interelement boundary. In the case of elements near the crack front, the asymptotically correct $1/\sqrt{r}$ type analytical solution is embedded in the boundary traction field. The developed procedure has been checked for its convergence properties by solving problems such as embedded penny shaped, or elliptical cracks in infinite domains, for which analytical solutions are available. Through this study, an optimum size of the elements near the crack front, as compared to the "characteristic length" of the crack, is also derived. The procedure was then applied to study the present class of problems.

While the present results for SIF were found to agree reasonably with the estimates of Kobayashi *et al.* for the case of semi-circular surface flaws, significant differences were found in the case of deep, oblong, semi-elliptical flaws at either outer or inner surfaces of thick walled pressurized cylinders. The possible reasons for these discrepancies will be discussed in the paper.

Due to length limitation, the paper will contain SIF solutions for pressurized cylinders of inner to outer diameter ratios of 4 : 5, 2 : 3 and 1 : 2, with pressurized and unpressurized inner semi-elliptical cracks of aspect ratios ($b/a=.1$, .2 and .5), at crack depths of $b/h=.5$ and .8; and with outer semi-elliptical flaws of similar geometries. Results for the above crack geometries in thermally-shocked cylinders will also be discussed.

1. Introduction: An important category of problems in thick-walled pressure vessels, especially those in nuclear reactor structural applications, is the presence of surface flaws, mostly of semi-elliptical geometries, either inside of the pressure vessel or outside of the pressure vessel. Presence of such surface flaws elevates the stresses considerably, increasing the possibility of failure of the pressure vessel. Thus the fracture analysis of such thick-walled pressure vessels is of utmost importance in assessing the structural integrity. Much prior work has not been done to investigate such problems, though some investigators have obtained approximate solutions using, for instance, two-dimensional analogs of these problems. Clifton et al [1] determined the critical stress-intensity factor for internally pressurized thick-walled vessels. Kobayashi et al [2,3,4] investigated several inner and outer semi-circular and semi-elliptical surface crack problems in internally pressurized and thermally shocked cylinders. Employing a conventional three-dimensional finite element program and virtual crack extension method, Blackburn and Hellen [5] obtained the solution for stress-intensity factors for surface cracks in blocks and cylinders. Recently Ayres [6] made an elastic three-dimensional analysis of semi-elliptical surface cracks subjected to thermal shocks and Hellen and Blackburn [7] calculated the stress-intensity factors, both using two- and three-dimensional conventional finite elements.

It has been well established that the singularity in stresses and strains due to the presence of flaws or cracks in structural components has to be specially treated in the analysis and solution procedures. In most of the previous works mentioned, either a conventional finite element solution procedure, which proves to be more expensive and less accurate; or highly approximate solution procedures such as the alternating method [2,3,4], with "correction" of flat plate solutions by "curvature correction factors" estimated from two-dimensional analogs, are used. When the crack is oblong and penetrates deeper into the thickness of the pressure vessel, a mere two-dimensional analog or a simple three-dimensional conventional finite element method may not be sufficient to assess the actual situation. In the solution procedures of Kobayashi [2,3,4] and Underwood [8], the effects of back surface on the crack were ignored and this may be very critical in the case of oblong cracks when the cracks penetrate deeper into the thickness of the pressure vessel wall. The solutions for stress-intensity factors for inner and outer surface cracks in pressurized vessels are obtained in the present paper through a newly developed, embedded singularity, three-dimensional hybrid-displacement finite element procedure with no restrictive assumptions, and the results are presented here for various aspect ratios of the ellipse, inner to outer diameter ratios and crack depth to thickness ratios. In the present procedure, the stress-intensity factors are computed directly instead of computing them indirectly such as from crack opening displacement method etc.

2. Formulation of the Problem: A brief description of the theoretical formulation of the three-dimensional, embedded singularity, hybrid-displacement finite element procedure is given here. The complete details of the mathematical formulation along with the assumed field functions can be found in references [9,10]. The accuracy, convergence and optimum size of the special singular element has been studied and well established [10,11].

The variational principle which governs the hybrid-displacement finite element model is the stationary condition of the modified total potential energy given below.

$$\bar{\Lambda}_{HD}(\underset{\sim}{u}, \underset{\sim}{v}, \underset{\sim L}{T}) = \sum_{m=1}^{N} \left\{ \int_{V_m} \left[\frac{1}{2} \underset{\sim}{\varepsilon}^T \underset{\approx}{E} \underset{\sim}{\varepsilon} - \bar{\underset{\sim}{F}}^T \underset{\sim}{u} \right] dV \right.$$

$$\left. + \int_{\partial V_m} \underset{\sim L}{T}^T (\underset{\sim}{u} - \underset{\sim}{v}) dS - \int_{S_{\sigma_m}} \bar{\underset{\sim}{T}}^T \underset{\sim}{v}\, dS \right\} \tag{1}$$

where N is the total number of finite elements; V_m is the volume of mth element; ∂V_m is the bounding surface of V_m; S_{σ_m} is that portion of ∂V_m where surface traction $\bar{\underset{\sim}{T}}$ is prescribed; $\underset{\approx}{E}$ is the elasticity tensor; $\bar{\underset{\sim}{F}}$ is the body force; $\underset{\sim}{u}$ is the arbitrary interior displacement field (which would contain the asynptotic variation of displacements for the elements near the crack front); $\underset{\sim}{v}$ is an inherently compatible interelement boundary displacement field; $\underset{\sim L}{T}$ are Lagrange multipliers (physically the boundary tractions) which are used to enforce the boundary displacement compatibility condition at the interelement boundary; and $\underset{\sim}{\varepsilon}$ are the strains derived from the interior displacement field function. The field functions are assumed as follows (subscript 's' denotes a "singular element", and subscript 'R' denotes a far field "regular element"):

$$\underset{\sim s}{u} = \underset{\approx R}{U}\, \underset{\sim}{\beta} + \underset{\approx a}{U} \begin{Bmatrix} K_I \\ K_{II} \\ K_{III} \end{Bmatrix} \; ; \; \underset{\sim R}{u} = \underset{\approx R}{U}\, \underset{\sim}{\beta}$$

$$\underset{\sim s}{v} = \underset{\approx s}{L}\, \underset{\sim}{q} \; ; \; \underset{\sim R}{v} = \underset{\approx R}{L}\, \underset{\sim}{q}$$

$$\underset{\sim Ls}{T} = \underset{\approx s}{R}\, \underset{\sim}{\alpha} \; ; \; \underset{\sim LR}{T} = \underset{\approx R}{R}\, \underset{\sim}{\alpha} \tag{2}$$

where $\underset{\approx R}{U}$ are arbitrary polynomial functions; $\underset{\approx a}{U}$ are asymptotic displacement solution functions; $\underset{\approx s}{L}$ are interpolates for boundary displacements; $\underset{\approx s}{R}$ are arbitrary functions for boundary tractions; $\underset{\sim}{\alpha}$ and $\underset{\sim}{\beta}$ are undetermined parameters; $\underset{\sim}{q}$ are the element nodal displacements; and K_I, K_{II} and K_{III} are the three stress-intensity factors. The field functions can be assumed such that the near field singular elements contain asymptotic solution and the far field regular elements do not contain asynptotic solution as given by eq. (2).

Substituting the assumptions of eq. (2) in eq. (1), and eliminating the undetermined parameters $\underset{\sim}{\alpha}$ and $\underset{\sim}{\beta}$ in terms of $\underset{\sim}{q}$ at the element level, the final system of algebraic matrix equations can be written as follows, the detailed derivation of which can be found in [10].

$$\begin{bmatrix} \underset{\approx}{K}_1 & \underset{\approx}{K}_2^T \\ \underset{\approx}{K}_2 & \underset{\approx}{K}_3 \end{bmatrix} \begin{Bmatrix} \underset{\sim}{q}^* \\ \underset{\sim}{K} \end{Bmatrix} = \begin{Bmatrix} \underset{\sim}{Q}_1 \\ \underset{\sim}{Q}_2 \end{Bmatrix} \tag{3}$$

where $\underset{\sim}{q}^*$ are the structure's nodal displacements; and $\underset{\sim}{K}$ are the stress-intensity factors for the three modes of crack extension at nodes along the crack front. As seen from eq. (3), the stress-intensity factors are directly solved for.

3.1 <u>Results and Discussions</u>: Fig. 1 gives the geometry of the internally pressurized thick-walled cylinder with semi-elliptical inner and outer surface cracks. The Poisson's ratio of the material is assumed to be 0.3. The length of the cylinder is assumed to be such that L/2a (and L/R_o) $\geq$ 3 for the finite element solution. Stress σ_{zz}, corresponding to the plane strain condition ($\sigma_{zz} = -\nu\ (\sigma_{RR} + \sigma_{\varphi\varphi})$) (where R and φ are the polar coordinates in the cross section of the cylinder) were imposed on the faces of the cylinder to account for the end condition of the problem. When the crack is at the inner surface of the pressure vessel, unpressurized as well as pressurized cracks are considered. The finite element breakdowns of the cylinder with inner and outer cracks are given in Fig. 2. Only one fourth of the cylinder needs to be modeled because of symmetry. The breakdown has 156 elements and 2670 total number of degrees of freedom.

3.2 Oblong Inner Semi-Elliptical Flaw: The solution for the stress-intensity factors for an oblong inner semi-elliptical flaw in a pressurized cylinder with geometric parameters b/a = 0.2, $b/(R_o - R_i) = 0.8$, $R_o/R_i = 1.5$ with crack surface pressure is given in Fig. 3. The value of σ_o used in the normalization procedure is given by $\sigma_o = \dfrac{2R_o^2P_i}{R_o^2-R_i^2}$. The result of the same problem estimated by Kobayashi [4] is also given in Fig. 1 and it can be seen that they are significantly different, though the two solutions agree well near the deepest penetration. In order to re-check the present result, the problem of pressurized inner semi-elliptical crack in a pressurized cylinder was solved again by removing the stresses $\sigma_{zz} = -\nu\ (\sigma_{RR} + \sigma_{\varphi\varphi})$ which was applied to simulate the plane strain condition, and enforcing the plane strain condition through supressing the displacements at corresponding faces. The result obtained for this case is also given in Fig. 3 by dotted lines and is very close to the result obtained by enforcing the plane strain condition through the stresses $\sigma_{zz} = -\nu\ (\sigma_{RR} + \sigma_{\varphi\varphi})$. The estimated value of stress-intensity magnification factor at the free surface ($\theta = 0^o$) is 2.26, which is about 1.7 times higher than that of Kobayashi [4] estimation, and at the deepest-penetration ($\theta = 90^o$) is 1.19 with a dip at $\theta = 45^o$. The solution for stress intensity factors for the same problem with no crack surface pressure is given in Fig. 4, wherein the value of σ_o used in the normalization procedure is given by $\sigma_o = P_i\ [(R_o/R_i)^2 + 1]\ /\ [(R_o/R_i)^2 - 1]$. The results are lower at all θ-locations as compared with the same problem with crack surface pressure and no comparative solution is given by Kobayashi [4].

3.3 Outer Semi-Elliptical Flaw: The results of the variation of K_I for an unpressurized outer semi-elliptical crack with geometric parameters, (b/a = 0.6; $R_o/R_i = 1.5$; $b/(R_o-R_i) = 0.4$) is shown in Fig. 5. The stress-intensity factor variation is normalized with respect to the closed form solution of an embedded elliptical flaw, the faces of which are acted on by a uniform pressure, σ_o, equal to the hoop stress at the outer face of the cylinder due to internal pressure P_i, v_{iz}, $\sigma_o = 2R_i^2P_i/(R_o^2-R_i^2)$.

The results estimated by Kobayashi [4] for an identical problem and by Blackburn and Hellen [5] for slightly different geometry ($R_o/R_i = 1.461$, whereas in the present case $R_o/R_i = 1.5$) are also given in Fig. 5. Again, as in the case of inner surface cracks, the computed stress-intensity magnification factor is maximum at the front surface ($\theta = 0^o$) and the magnification factor decreases continuously with increasing elliptical angle θ. The actual stress-intensity factor at $\theta = 0^o$ is only about 1.5 percent lower than the stress-intensity factor at $\theta = 90^o$. As it can be seen from Fig. 5, the comparison of the present directly computed result with that of Kobayashi [4] and Blackburn's [5] solution, the present result agrees reasonably well with Blackburn's solution throughout except for first 10 degrees of the elliptical angle. However, Kobayashi's solution seems to differ significantly from the other two solutions. The 13 percent difference in stress-intensity magnification factor between present and Blackburn's solution at the free surface ($\theta = 0^{o}$) could be attributed to the indirect solution procedure, ie, through the virtual crack extension method, and slight difference in the geometry of the problem in [5]. Thus, it appears that the method of estimation of stress-intensity factor in [4], through the solution for surface flaws in the flat plates modified by curvature correction factor is questionable.

3.4 Outer Semi-Circular Flaws: The results of the variation of stress-intensity factors for unpressurized semi-circular crack with geometric parameters, ($b/a = 1$, $R_o/R_i = 1.5$) and two depth to thickness ratios 0.6 and 0.8 are given in Fig. 6 and Fig. 7 respectively. The value of σ_o used in the normalization procedure is also given by $\sigma_o = 2R_i^2 P_i/(R_o^2-R_i^2)$. The qualitative features of these two problems are also similar to the inner as well as outer semi-elliptical crack problems discussed before. With all the geometric parameters, except the ratio of crack depth to the thickness of the thick-walled cylinder, kept constant, one can observe the effect of increased stress-intensity magnification factor at all θ-locations for a deeper crack from Figs. 6 and 7. The comparative estimates of Kobayashi [4] are also shown in Figs. 6 and 7 and again were found to differ significantly for these problems.

4. Conclusions: The solutions by the present procedure are found to be in reasonable agreement with those obtained through conventional finite element method, such as those of Blackburn and Hellen [5]. The procedure used by Kobayashi et al [4], namely the alternating method for flat plates with "curvature corrections" to account for cylindrical geometry, gave excellent correlation with the solutions obtained by the present hybrid-displacement model in the case of pressurized and unpressurized semi-circular inner surface flaws in a pressurized cylinder [12]. But in the present case of oblong semi-elliptical flaws and cracks penetrating deeper into the thickness, the alternating method used by Kobayashi [4] fails to yield results comparable to the present. The procedure in [4] may not be valid for cases of crack depths in which the effects of back surface had to be considered. Again in the alternating solution procedure of [4] the hoop stress variation along the thickness direction of the thick-walled cylinder was approximated by polynomials, and since the solution of embedded elliptical crack in an infinite solid (needed in the alternating method) is available for only a limited class of polynomial crack pressure distributions, the above polynomial fitting of actual stresses may not be accurate enough. Moreover in the case of oblong and deeper semi-elliptical surface cracks, a simple two-dimensional analog employing various curvature correction factors may not be an adequate modeling of a complex three-dimensional problem and may be questionable.

Results for other crack aspect ratios, and cylinder ratios are not included in the present paper due to conference imposed page limitations.

Acknowledgements: The present results were obtained during the course of an investigation supported by the National Science Foundation, under grant NSF ENG-74-21346 to the Georgia Institute of Technology.

References

[1]. Clifton, R. J., Simonson, E. R., Jones, A. F., and Green, S. J., "Determination of the Critical Stress-Intensity Factor K_{I_c} for Internally Pressurized Thick-Walled Vessels," SESA paper No. 2407A, May 1975, and to be published in Experimental Mechanics.

[2]. Kobayashi, A. S., Polvanich, N., Emery, A. F., and Love, W. J., "Stress-Intensity Factor of a Surface Crack in a Pressurized Cylinder," Computational Fracture Mechanics, (edited by E. F. Rybicki and S. E. Benzley), ASME, pp. 121-132 (1975).

[3]. Kobayashi, A. S., Emery, A. F., Polvanich, N., and Love, W. J., "Surface Flaw in a Pressurized and Thermally Shocked Hollow Cylinder," paper G-4/3, 3rd SMIRT, University of London, Sept. 1975.

[4]. Kobayashi, A. S., Emery, A. F., Polvanich, N., and Love, W. J., "Inner and Outer Surface Cracks in Internally Pressurized Cylinders," presented at Joint Conference on Pressure Vessels and Pipings and Petroleum Mechanical Engineering, Mexico City, Sept. 1976 and published in ASME Transactions.

[5]. Blackburn, W. S., and Hellen, T. K., "Calculation of Stress-Intensity Factors for Elliptical and Semi-Elliptical Cracks in Blocks and Cylinders," Central Electricity Generating Board Report No. RD/B/N3103, UK, July 1974.

[6]. Ayres, D. J., "Three-Dimensional Elastic Analysis of Semi-elliptical Surface Cracks Subject to Thermal Shocks," Computational Fracture Mechanics, (edited by E. F. Rybicki and S E. Benzley), ASME, pp. 133-143 (1975).

[7]. Hellen, T. K., and Blackburn, W. S., "The Calculation of Stress-Intensity Factors in Two- and Three-Dimensions Using Finite Elements," Computational Fracture Mechanics, (edited by E. F. Rybicki and S. E. Benzley), ASME, pp. 103-120 (1975).

[8]. Underwood, J. H., "Stress-Intensity Factors for Internally Pressurized Thick-Walled Cylinders," Stress Analysis and Growth of Crack, ASTM STP-513, pp. 59-70 (1972).

[9]. Atluri, S. N., Kathiresan, K., and Kobayashi, A. S., "Three-Dimensional Linear Fracture Mechanics Analysis by a Displacement-Hybrid Finite Element Model," paper L-7/3, 3rd SMIRT, University of London, Sept. 1975.

[10]. Kathiresan, K., "Analysis of Three-Dimensional Fracture Problems by a Displacement-Hybrid Finite Element Method," Ph.D. Thesis, Georgia Institute of Technology, Sept. 1976.

[11]. Atluri, S. N., Kathiresan, K., "On a 3-D 'Singularity Element' for Computation of Combined-Mode Stress-Intensities," NASA Special Technical Publications (Proceedings of 13th SES Meeting), pp. 257-264 (1976).

[12]. Atluri, S. N., Kathiresan, K., Kobayashi, A. S., and Nakagaki, M., "Inner Surface Cracks in an Internally Pressurized Cylinder Analyzed by a Three Dimensional Displacement-Hybrid Finite Element Method," to be presented at the 3rd International Conference on Pressure Vessel Technology, Tokyo, Japan, April 1977.

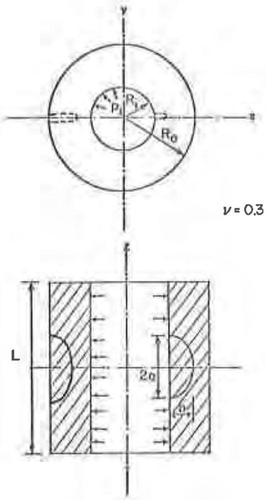

FIG 1 : Inner and Outer Semi-Elliptical Cracks in a Pressurized Cylinder.

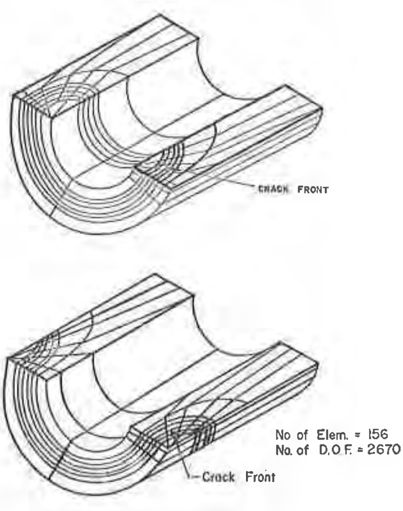

FIG 2 : Finite Element Breakdown for Inner and Outer Crack Problems.

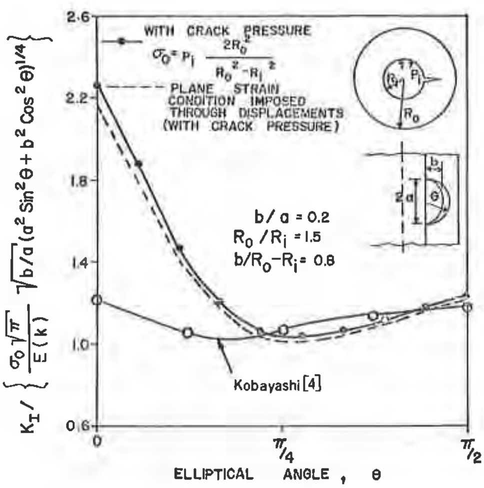

FIG. 3 : Stress Intensity Magnification Factor for an Oblong Inner Semi-Elliptical Crack in a Pressurized Cylinder

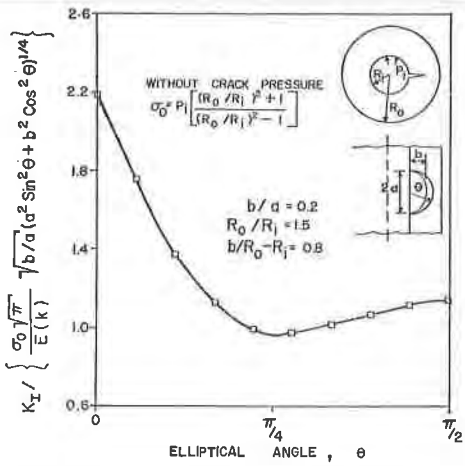

FIG. 4 : Stress Intensity Magnification Factor for an Oblong Inner Semi-Elliptical Crack in a Pressurized Cylinder

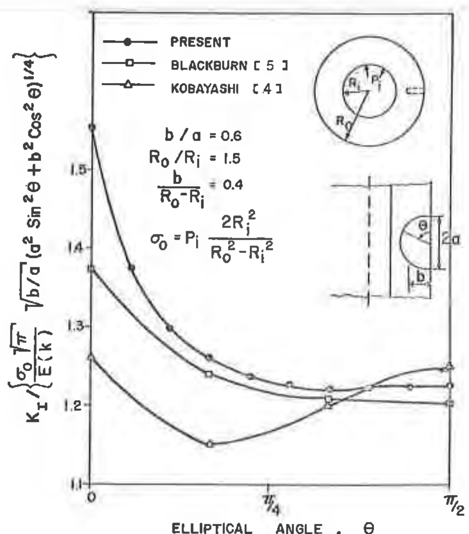

FIG. 5 : Stress Intensity Magnification Factor for an Outer Semi-Elliptical Crack in a Pressurized Cylinder

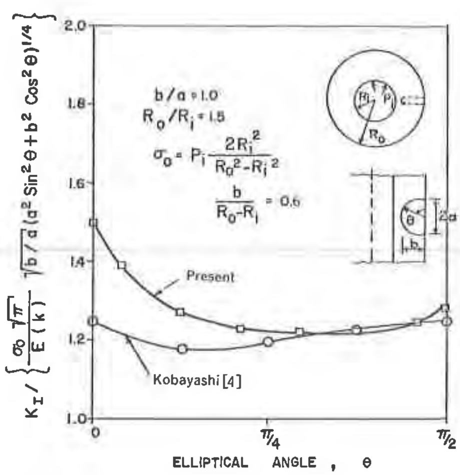

FIG. 6 : Stress Intensity Magnification Factor for Outer Semi-Circular Cracks in a Pressurized Cylinder

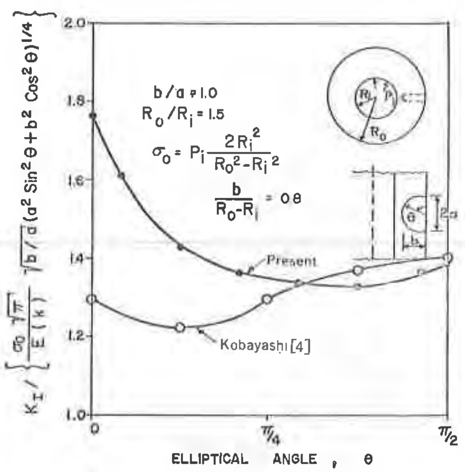

FIG. 7 : Stress Intensity Magnification Factor for Outer Semi-Circular Cracks in a Pressurized Cylinder